Electronic Supporting Information on

Slow magnetic relaxation and strong magnetic coupling in the nitroxyl radical complexes of Ln(III) with diamagnetic ground state (Ln = Lu, Eu)

Lorenzo Sorace,[a] Alexey A. Dmitriev,[b] Mauro Perfetti [a] and Kira E. Vostrikova [c]**

[a]Department of Chemistry U. Schiff, University of Florence and INSTM Research Unit. Via della Lastruccia 3-13, Sesto Fiorentino 50019, Firenze (IT). ORCID: 0000-0001-5649-0449

[b]Voevodsky Institute of Chemical Kinetics and Combustion, Siberian Branch, Russian Academy of Sciences, 630090 Novosibirsk, Russia.

[c]Nikolaev Institute of Inorganic Chemistry, Siberian Branch, Russian Academy of Sciences.

Table S1. Crystallographic data and refinement details for the compounds [LnRad$(NO_3)_3$] (Ln = Eu, Lu).

	Eu	**Lu**
Empirical formula	$C_{15}H_{16}N_6O_{11}Eu$	$C_{15}H_{16}N_6O_{11}Lu$
Formula weight	608.29	631.29
Space group	$P2_1/n$	$P2_1/n$
a/Å	10.0737(2)	9.9511(2)
b/Å	16.5107(4)	16.4632(4)
c/Å	12.7562(2)	12.8156(3)
β/°	104.639(1)	104.088(1)
Volume/Å^3	2052.79(8)	2036.39(8)
Z	4	4
Temperature	100	150
$\rho_{calc}g/cm^3$	1.968	2.059
μ/mm^{-1}	3.13	4.92
F(000)	1196.979	1228.362
Crystal size/mm^3	0.1 × 0.05 × 0.03	0.35 × 0.1 × 0.1
2Θ range for data collection/°	4.066 to 51.418	2.05 to 30.50
Index ranges	-14 ≤ h ≤ 17, -29 ≤ k ≤ 29, -22 ≤ l ≤ 22	-13 ≤ h ≤ 14, -19 ≤ k ≤ 21, -17 ≤ l ≤ 16
T_{min}, T_{max}	0.56, 0.75	0.643, 0.746
Reflections collected	52996	16819
Independent reflections	12193	4929
observed [$I \geq 2u(I)$] reflections	7299	4513
R_{int}, $(\sin\theta/\lambda)_{max}$ (Å^{-1})	0.088, 0.893	0.028, 0.714
$R[F^2 > 2\sigma(F^2)]$, $wR(F^2)$	0.055, 0.120	0.033, 0.129, 0.94
Restraints/parameters	0/300	6/300
H-atom treatment	H-atom parameters constrained	
	$w = 1/[\sigma^2(F_o^2) + (0.0466P)^2]$ where $P = (F_o^2 + 2F_c^2)/3$	$w = 1/[\sigma^2(F_o^2) + (0.P)^2 + 64.6601P]$ where $P = (F_o^2 + 2F_c^2)/3$
$\Delta\rho_{max}$, $\Delta\rho_{min}$ (e Å^{-3})	4.95, −5.52	2.68, −2.73
Goodness-of-fit on F^2	1.060	0.94
Largest diff. peak/hole / *e Å^{-3}*	2.4/-1.1	2.68/-2.73

Table S2. Geometry analysis of the complexes by SHAPE* software.

	Temperature of RXD experiment, K	Spherical tricapped trigonal prism, D_{3h}	Spherical capped square antiprism, C_{4v}	Muffin, C_s
[Eu(Tpm)(NO_3)$_3$]	150	2.05	2.910	3.027
[Eu(Rad)(NO_3)$_3$]	100	2.385	3.191	3.338
[Y(Rad)(NO_3)$_3$]	295	2.141	2.935	3.171
[Dy(Rad)(NO_3)$_3$]	295	2.220	3.025	3.256

*SHAPE 2.1 program for the stereochemical analysis of molecular fragments by means of continuous shape measures and associated tools. http://www.ee.ub.edu/]

Table S3. Selected bond lengths (Å) in coordination sphere of the compounds [LnRad(NO_3)$_3$], Ln = Eu, Lu.

Eu		**Lu**	
Bond	Length	Bond	Length
Eu1—O2	2.424 (2)	Lu1—O2	2.3351 (13)
Eu1—O4	2.445 (3)	Lu1—O3	2.3719 (14)
Eu1—O5	2.488 (3)	Lu1—O4	2.3899 (15)
Eu1—O6	2.425 (2)	Lu1—O5	2.3490 (14)
Eu1—O7	2.489 (3)	Lu1—O6	2.3989 (15)
Eu1—O8	2.433 (2)	Lu1—O7	2.3750 (14)
Eu1—O9	2.466 (2)	Lu1—O8	2.3611 (15)
Eu1—N2	2.531 (3)	Lu1—N2	2.4373 (16)
Eu1—N3	2.533 (3)	Lu1—N3	2.4319 (16)
N1—O2	1.242 (2)	N1—O2	1.276 (2)

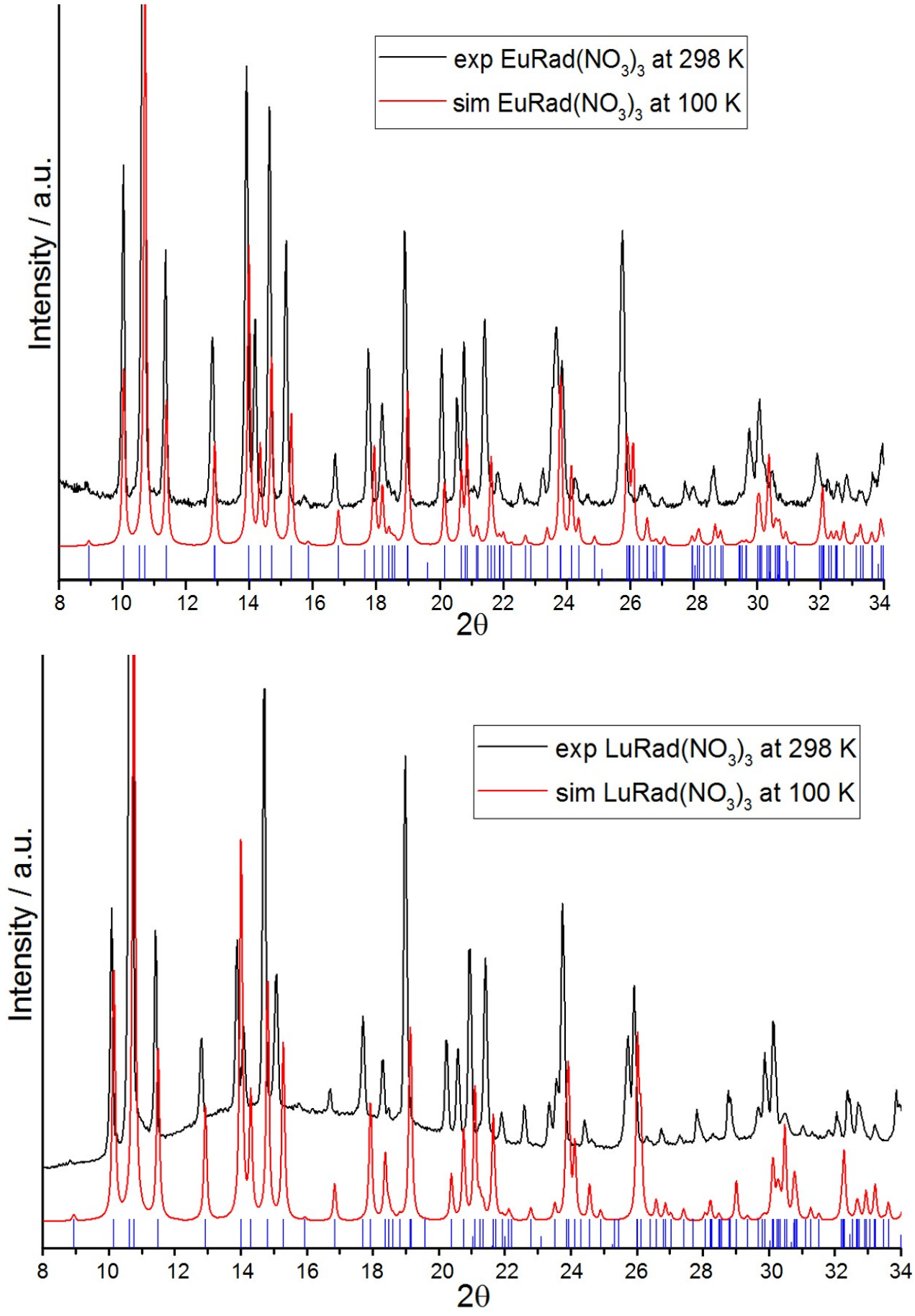

Figure S1. Simulated (red) and experimental (black) powder patterns of the compounds [LnRad$(NO_3)_3$].

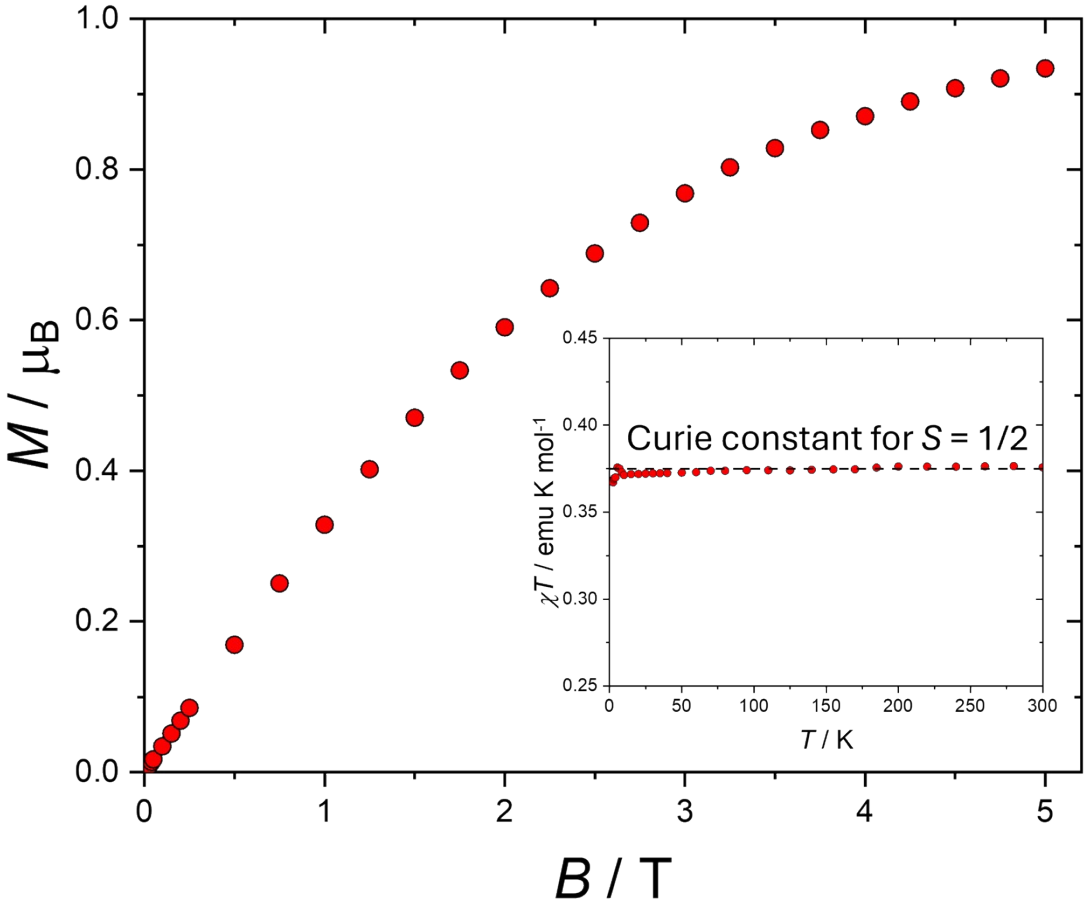

Figure S2. Magnetic behavior of [LuRad$(NO_3)_3$]: magnetization curve measured at 2 K and temperature dependence of χT product (inset) at B = 1 T.

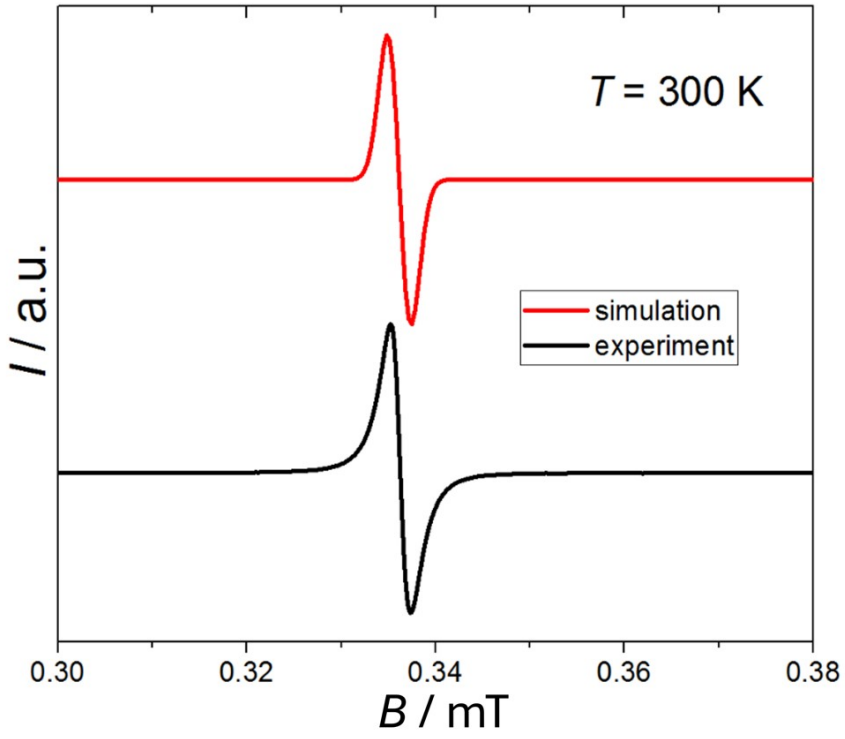

Figure S3. The powder X-band EPR spectrum of [LuRad$(NO_3)_3$] at T=300K with its simulation using an isotropic g=1.998(1).

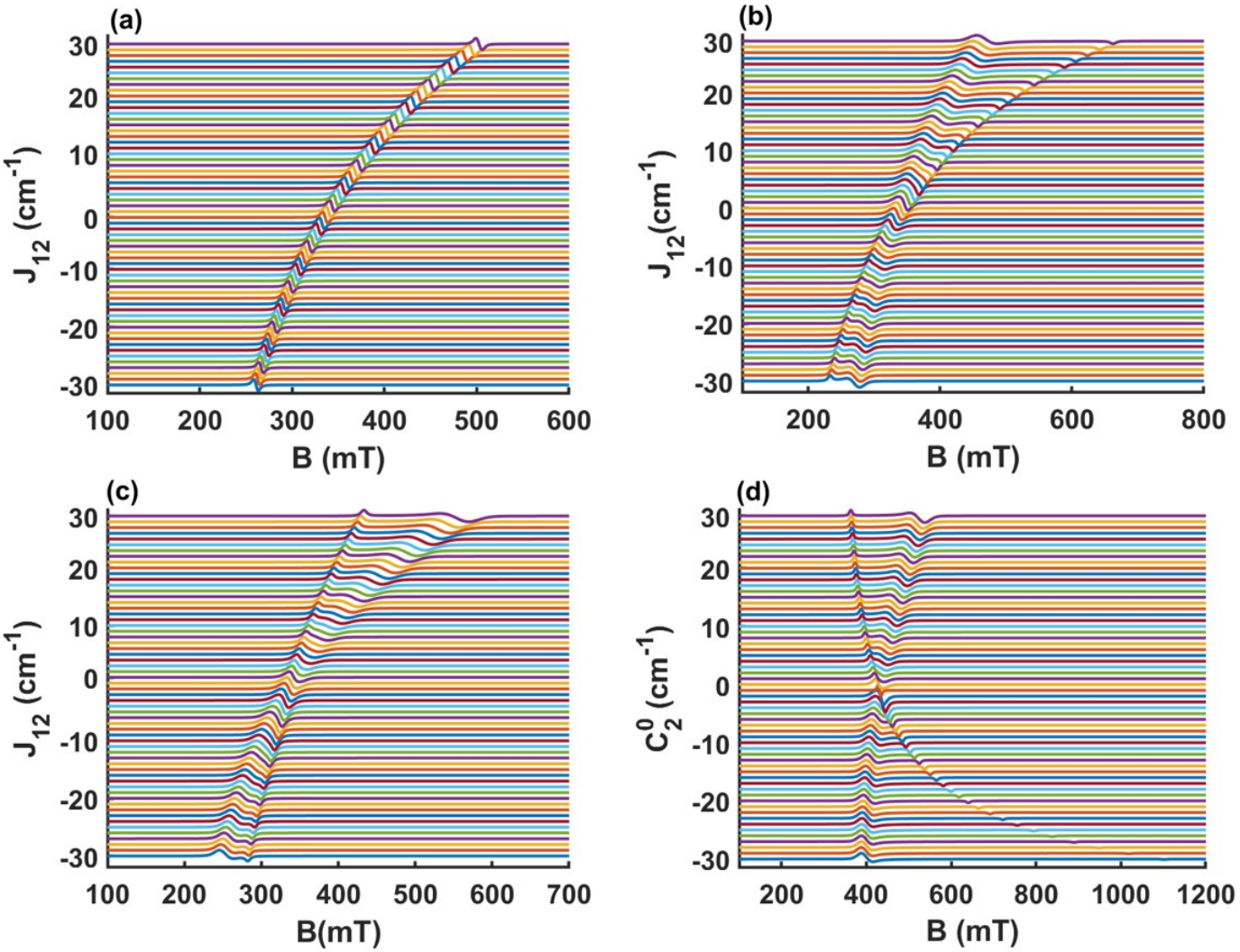

Figure S4 Survey of the simulated EPR spectra (ν = 9.39 GHz, T= 5 K) as a function of different parameters. a) $C_2^0 = 0$ and J varying from -30 cm^{-1} (ferromagnetic) to +30 cm^{-1} (antiferromagnetic) b) C_2^0=-10 cm^{-1} and J_{12} varying from -30 cm^{-1} (ferromagnetic) to +30 cm^{-1} (antiferromagnetic) c) C_2^0=+10 cm^{-1} and J_{12} varying from -30 cm^{-1} (ferromagnetic) to +30 cm^{-1} (antiferromagnetic) d) J_{12} = +20 cm^{-1} (antiferromagnetic) and C_2^0 varying from -30 cm^{-1} to +30 cm^{-1}.

EPR Simulation

Spin structure used for the Easy Spin script:
Sys.S=[3 3 ½];
Sys.g=[gfree 1 1.998];
Sys.B_2=[0 ;14; 0]*clight*10^{-4};
Sys.J=[370 19.5 0] *clight*10^{-4};
Sys.lw=[1 6];
Sys.HStrain=[600 600 100];

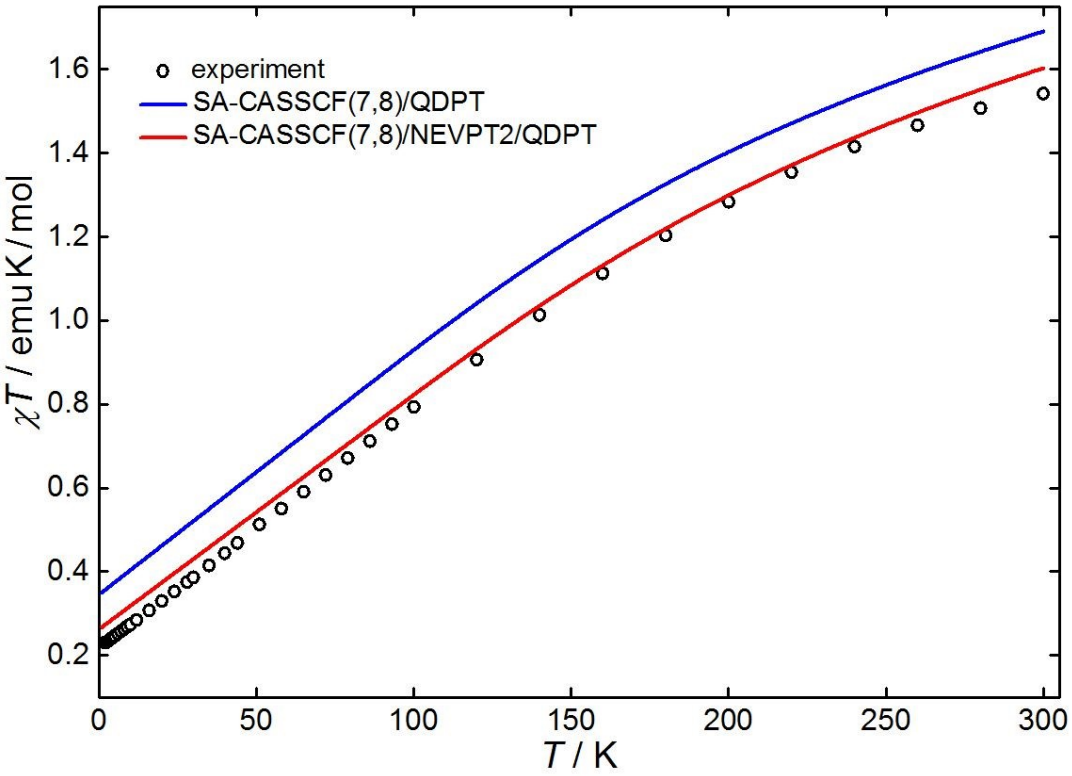

Figure S5. Temperature dependence of magnetic susceptibility for [EuRad$(NO_3)_3$]: experiment (circles) and *ab initio* calculations, SA-CASSCF(7,8)/QDPT (blue) and SA-CASSCF(7,8)/NEVPT2/QDPT (red).

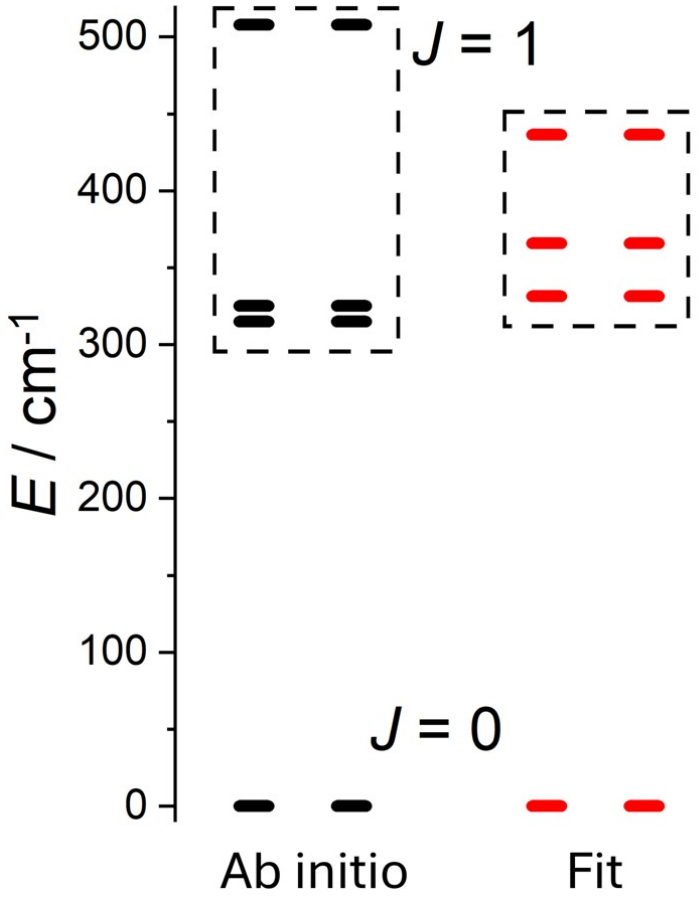

Figure S6. Visual comparison of the energy level structure of the ground and first excited multiplet of [EuRad$(NO_3)_3$], obtained from the experimental magnetic and EPR data fit and *ab initio* (see below). The doubly degenerate nature of the states in zero field stems from the coupling between the Eu^{3+} ion and Rad.

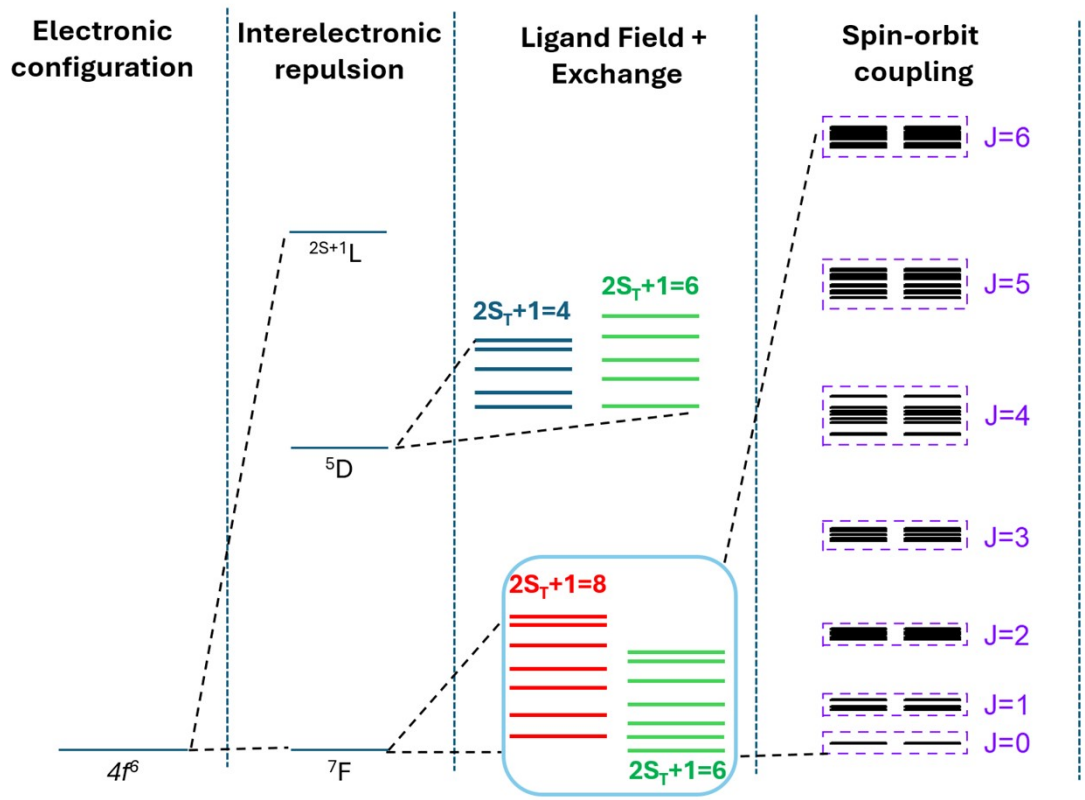

Figure S7 Plot of the different electronic energy terms for [EuRad$(NO_3)_3$] included in the calculations. Energy is not in scale.

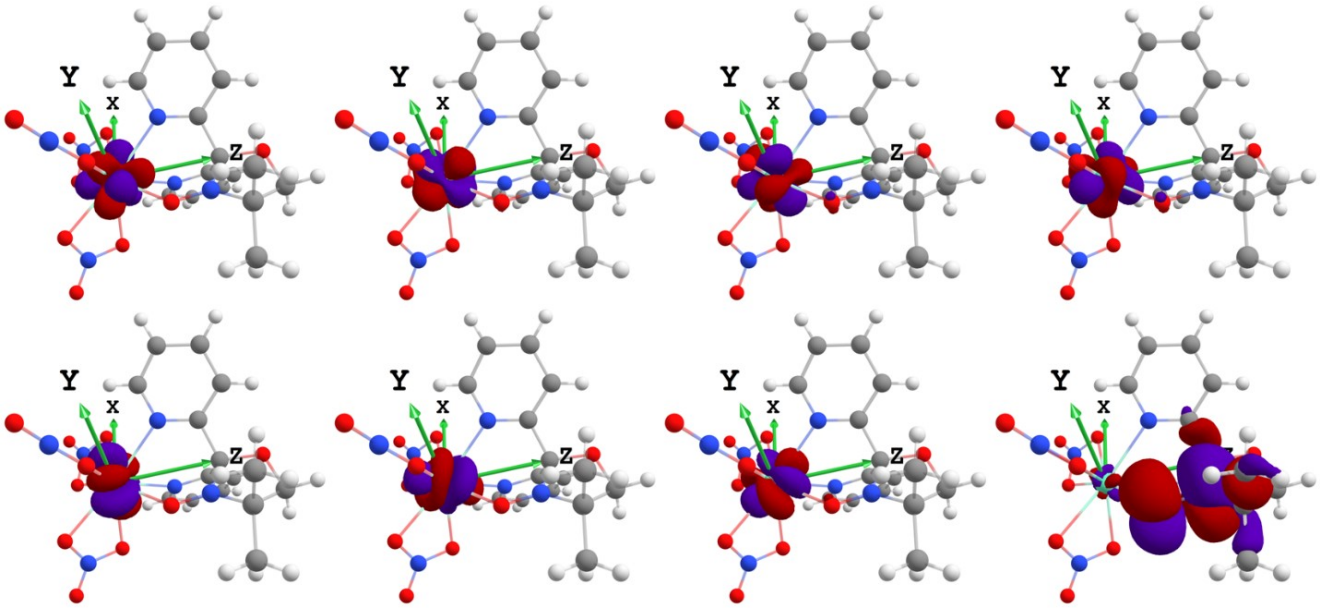

Figure S8. MOs involved in the active space of the SA-CASSCF(7,8) calculations on complex [EuRad$(NO_3)_3$] (7 octets, 12 sextets and 5 quartets were involved in the SA). Geometry corresponds to the SCXRD structure at 100 K.

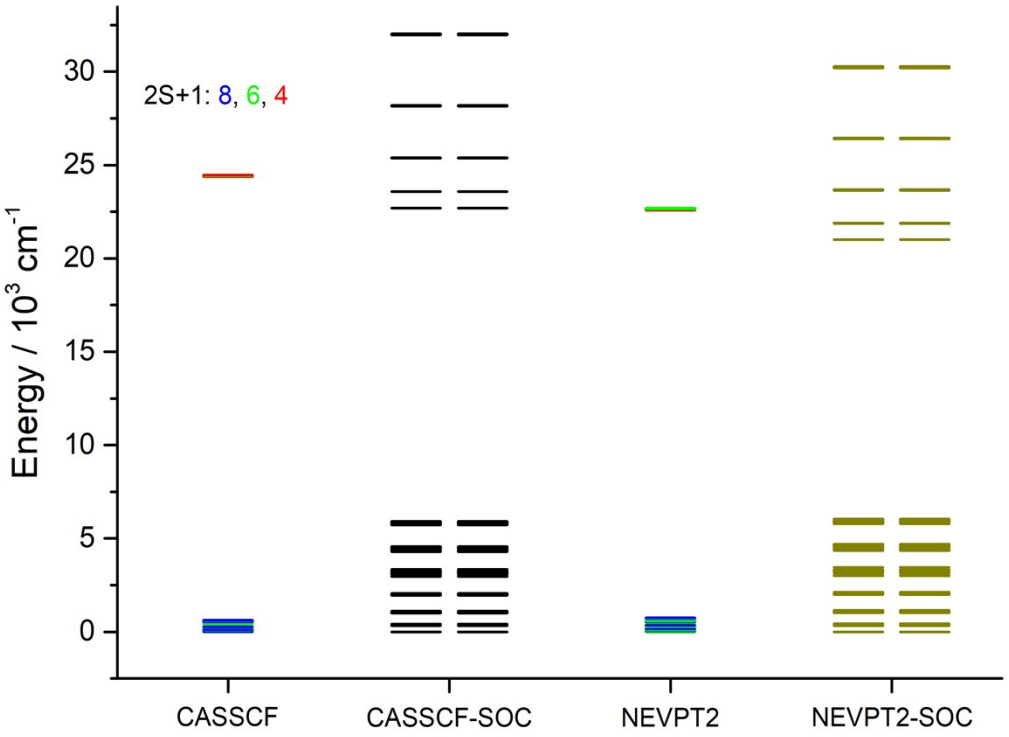

Figure S9. Relative states energies of [EuRad$(NO_3)_3$] calculated at SA-CASSCF(7,8) (CASSCF), SA-CASSCF(7,8)/QDPT (CASSCF-SOC), SA-CASSCF(7,8)/NEVPT2 (NEVPT2) and SA-CASSCF(7,8)/NEVPT2/QDPT (NEVPT2-SOC) levels of theory with 7, 12 and 5 roots for the multiplicities of 8 (blue), 6 (green) and 4 (red), correspondingly.

Table S4. Lowest octets and sextets after SA-CASSCF(7,8) calculations (7 octets, 12 sextets, 5 quintets) with their energies and contributions (> 0.1) of different electronic configurations to the wavefunction of each root.

Octets				Sextets			
Root	Energy, Eh	Contribution	Electronic configuration	Root	Energy, Eh	Contribution	Electronic configuration
0	-12562.7830773	0.89166	11111110[a]	0	-12562.783133	0.84855 0.10606	11111110 [a] 11111101
1	-12562.782621	0.89100	11111101	1	-12562.782697	0.84936 0.11577	11111101 11111110
2	-12562.781904	0.96640	11111011	2	-12562.781994	0.94191	11111011
3	-12562.781218	0.70813 0.19771	11110111 11101111	3	-12562.781243	0.62144 0.17981 0.14473	11110111 11011111 11101111
4	-12562.780912	0.89390	11011111	4	-12562.780934	0.71024 0.11991	11011111 10111111
5	-12562.780718	0.41834 0.28881 0.25590	11101111 10111111 11110111	5	-12562.780800	0.38237 0.29453 0.23064	11101111 11110111 10111111
6	-12562.780327	0.64146 0.33765	10111111 11101111	6	-12562.780377	0.59351 0.36540	10111111 11101111

[a] 1st number – radical ligand SOMO, 2-8 numbers – europium 4f-orbitals.

Table S4 presents the lowest seven octets and sextets with the contributions of different electronic configurations to the wavefunction of each root. Most of them have dominant contribution of one electronic configuration, and only fifth octet and fifth sextet have stronger multireference nature with close contributions of three configurations. SOMO of radical is always populated by one electron and the difference in configurations is defined by redistribution of electrons between seven 4f-orbitals of europium. The wavefunctions of the highest five sextets and quartets have much stronger multireference nature with bunch of different configurations with contributions lower than 10%. After account of SOC in QDPT approach, the energy levels are Kramers doublets, the lowest states can be roughly grouped as a result of interaction between the Eu(III) states with full moment J=0-6 after split in the ligand field and doublet of radical ligand (Figure S9, purple designations). The wavefunctions of these spin-free states are the combination of number of states with different M_s and weights of their contributions are rather small, no more that 10-15 %.

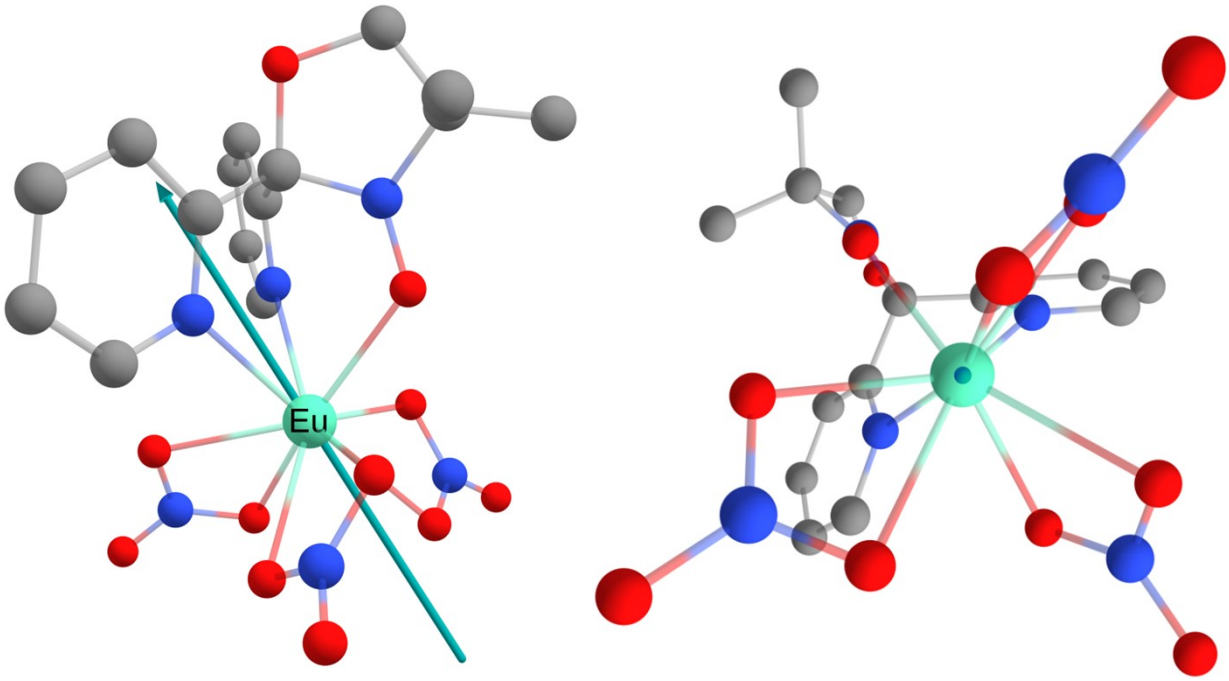

Figure S10. The orientation of the *ab initio* calculated main magnetic axis (teal vector) of the ground Kramers doublet for [EuRad$(NO_3)_3$] complex. The view along the main magnetic axis (right). The hydrogens are omitted.

Table S5. Angles between the main magnetic axes of excited Kramers doublets and the main magnetic axis of the ground state Kramer doublet (KD) calculated for [EuRad$(NO_3)_3$].

KDs	1	2	3	4	5	6	7	8	9
∠, °	0	96.6	10.2	27.6	95.3	23.1	17.6	49.3	65.5

Table S6. Principal values of g-tensor of *nine* lowest Kramers doublets with the direction of the main magnetic axes.

KD	Principal values		Main Magnetic Axes			
				x	y	z
1	g_X	1.58658	Xm	-0.467008	0.820432	0.329839
	g_Y	1.64033	Ym	-0.753578	-0.564424	0.336966
	g_Z	1.77790	Zm	0.462627	-0.091193	0.881850
2	g_X	1.13170	Xm	0.390610	-0.004972	0.920543
	g_Y	1.63800	Ym	0.792705	0.510219	-0.333610
	g_Z	2.28735	Zm	-0.468020	0.860030	0.203239
3	g_X	1.72106	Xm	-0.489338	0.858319	0.154393
	g_Y	2.11457	Ym	-0.802109	-0.512447	0.306625
	g_Z	2.68229	Zm	0.342301	0.026203	0.939225
4	g_X	2.01471	Xm	0.709929	0.106676	-0.696147
	g_Y	2.03138	Ym	0.233668	0.896792	0.375717
	g_Z	2.10975	Zm	0.664379	-0.429399	0.611732
5	g_X	1.65478	Xm	0.839347	0.005668	-0.543566
	g_Y	1.54038	Ym	0.040171	0.996565	0.072422
	g_Z	0.42156	Zm	0.542109	-0.082623	0.836236
6	g_X	1.20483	Xm	-0.688982	-0.355462	0.631625
	g_Y	1.45308	Ym	0.452707	-0.891624	-0.007966
	g_Z	3.13812	Zm	0.566003	0.280453	0.775233
7	g_X	2.84594	Xm	0.536024	0.200030	0.820162
	g_Y	2.09875	Ym	0.575316	0.624432	-0.528296
	g_Z	1.31875	Zm	-0.617811	0.755031	0.219630
8	g_X	1.60636	Xm	-0.793362	-0.461300	-0.397215
	g_Y	2.07256	Ym	0.484735	-0.873441	0.046192
	g_Z	2.91372	Zm	-0.368252	-0.155897	0.916563
9	g_X	2.90094	Xm	0.631743	-0.772924	0.059062
	g_Y	2.68506	Ym	0.770056	0.634489	0.066613
	g_Z	2.00105	Zm	-0.088961	0.003398	0.996029

Table S7. Topological properties (a.u.) of the electron density computed at BCP's for the presented bonds in [EuRad$(NO_3)_3$] complex. The wavefunction after ***SA-CASSCF(7,8)*** calculation was used for the analysis.

Bond	d, Å	P	$\rho(r)$	$\nabla^2\rho(r)$	$H(r)$	$\lvert V(r)\rvert/G(r)$	ε	η
Eu-O_{trip}	2.424	0.19	0.046	0.215	2.9e-4	0.994	0.0442	0.1813
Eu-$N1_{trip}$	2.534	0.20	0.044	0.161	-1.7e-3	1.041	0.0397	0.2022
Eu-$N2_{trip}$	2.531	0.21	0.044	0.162	-1.8e-3	1.041	0.0373	0.2021
Eu-O1	2.444	0.34	0.047	0.204	-1.3e-3	1.025	0.0650	0.1898
Eu-O2	2.489	0.33	0.042	0.186	-1.3e-4	1.003	0.0519	0.1854
Eu-O3	2.425	0.37	0.049	0.214	-1.8e-3	1.032	0.0811	0.1919
Eu-O4	2.489	0.30	0.042	0.187	5e-5	0.999	0.0531	0.1836
Eu-O5	2.433	0.35	0.048	0.210	-1.7e-3	1.031	0.0821	0.1919
Eu-O6	2.464	0.32	0.045	0.197	-6.3e-4	1.013	0.0633	0.1880

P – Mayer bond order; $\rho(r)$ – electron density; $-\nabla^2\rho(r)$ Laplacian of the electron density; $H(r)$ – total energy density; $V(r)$ – potential energy density; $G(r)$ – Lagrangian kinetic energy density; ε – ellipticity of electron density; η – eta index.

Table S8. Topological properties (a.u.) of the electron density computed at BCP's for the presented bonds in [Eu(Tpm)$(NO_3)_3$] complex. The wavefunction after ***SA-CASSCF(6,7)*** calculation was used for the analysis.

Bond	d, Å	P	$\rho(r)$	$\nabla^2\rho(r)$	$H(r)$	$\lvert V(r)\rvert/G(r)$	ε	η
Eu-$N1_{trip}$	2.672	0.1	0.032	0.117	6.1e-4	0.979	0.0610	0.1940
Eu-$N2_{trip}$	2.663	0.1	0.032	0.120	6.2e-4	0.979	0.0569	0.1928
Eu-$N3_{trip}$	2.655	0.1	0.033	0.122	4.8e-4	0.984	0.0696	0.1947
Eu-O1	2.497	0.34	0.042	0.180	-0.7e-4	1.002	0.0726	0.1877
Eu-O2	2.509	0.31	0.040	0.176	2.7e-4	0.994	0.0480	0.1853
Eu-O3	2.480	0.33	0.043	0.187	-4.7e-4	1.010	0.0712	0.1903
Eu-O4	2.536	0.34	0.038	0.165	8.6e-4	0.979	0.0336	0.1797
Eu-O5	2.459	0.33	0.046	0.197	-9.9e-4	1.020	0.0732	0.1909
Eu-O6	2.500	0.29	0.041	0.180	1.6e-4	0.996	0.054	0.1858

P – Mayer bond order; $\rho(r)$ – electron density; $-\nabla^2\rho(r)$ Laplacian of the electron density; $H(r)$ – total energy density; $V(r)$ – potential energy density; $G(r)$ – Lagrangian kinetic energy density; ε – ellipticity of electron density; η – eta index.

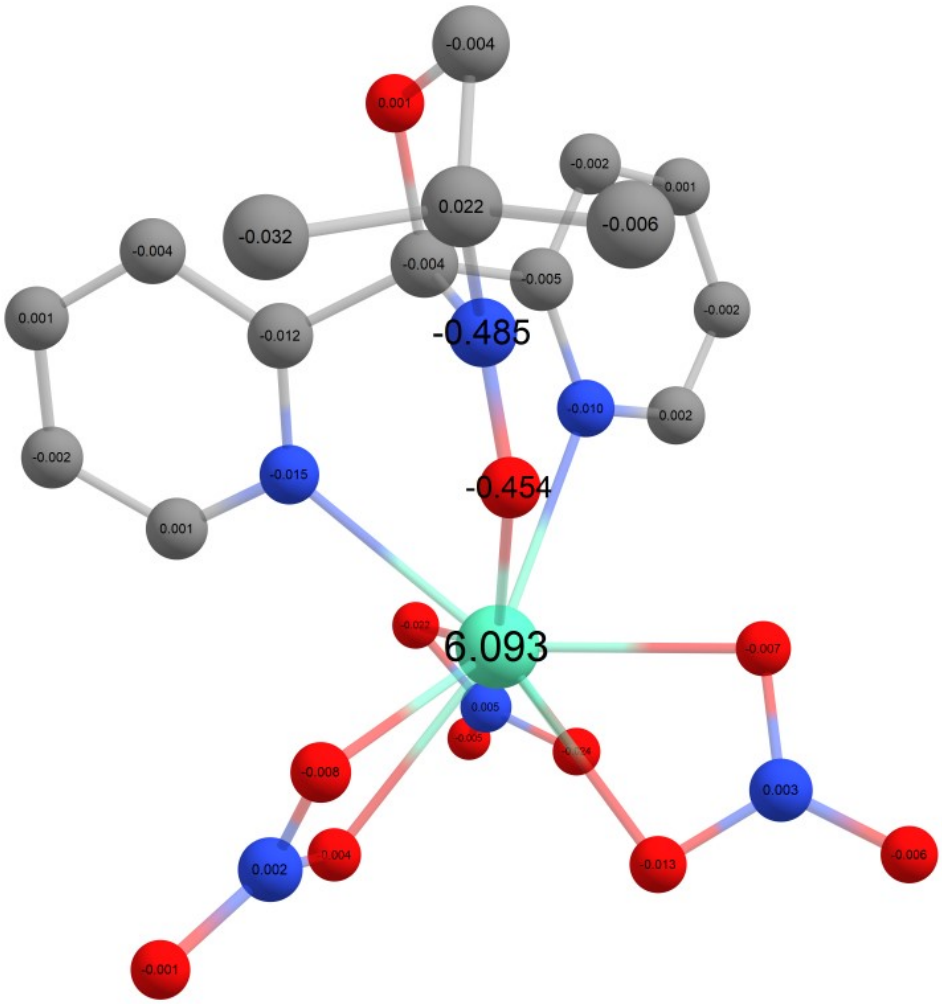

Figure S11. Spin density map for [EuRad(NO_3)$_3$] calculated for the ground sextet at UB3LYP/def2-TZVP level with SARC2-DKH-QZVP basis set for Eu and relativistic DKH2 Hamiltonian.

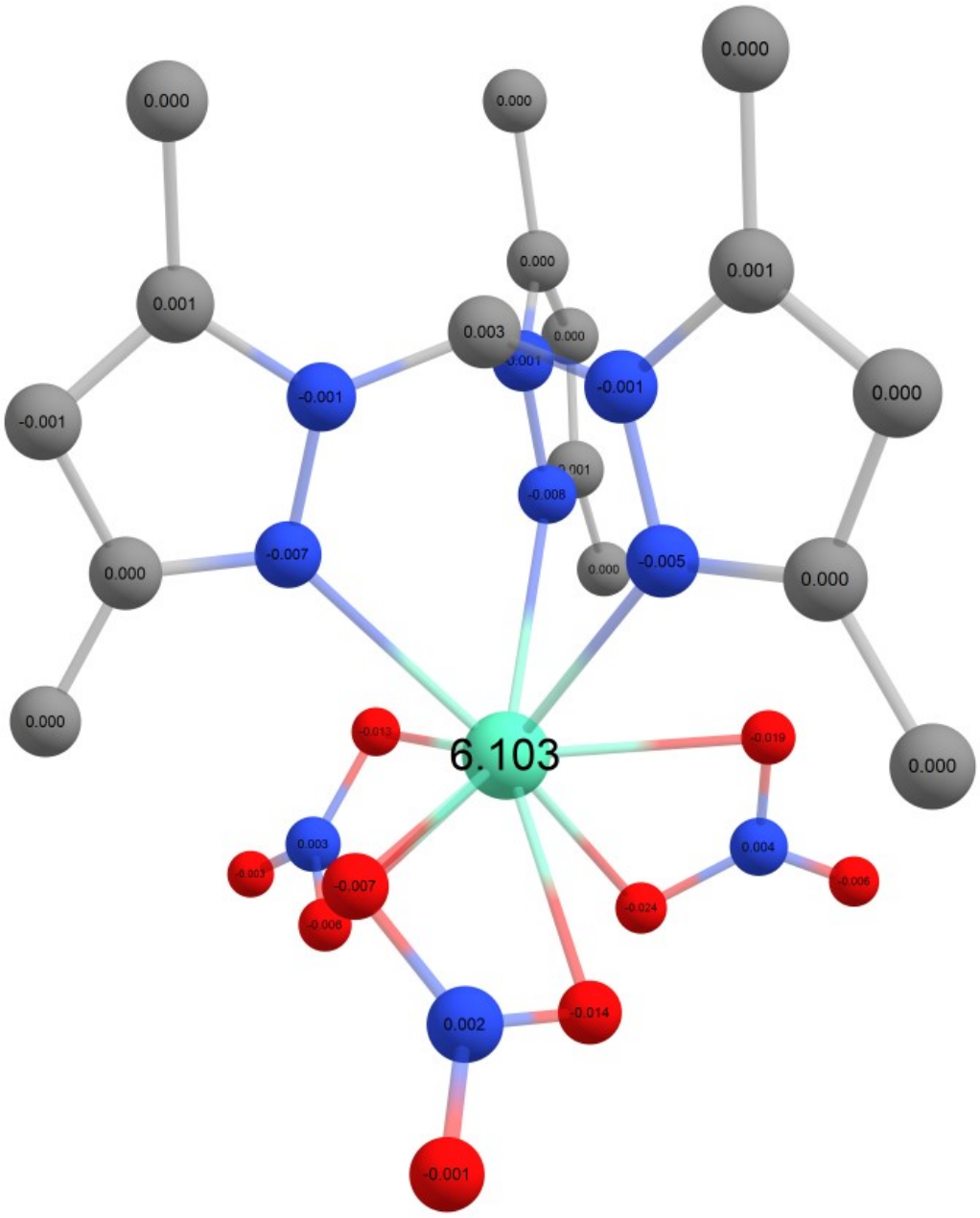

Figure S12. Spin density map for the [Eu(Tpm)(NO_3)$_3$] complex calculated in the ground septet at UB3LYP/def2-TZVP level with SARC2-DKH-QZVP basis set for Eu and relativistic DKH2 Hamiltonian.

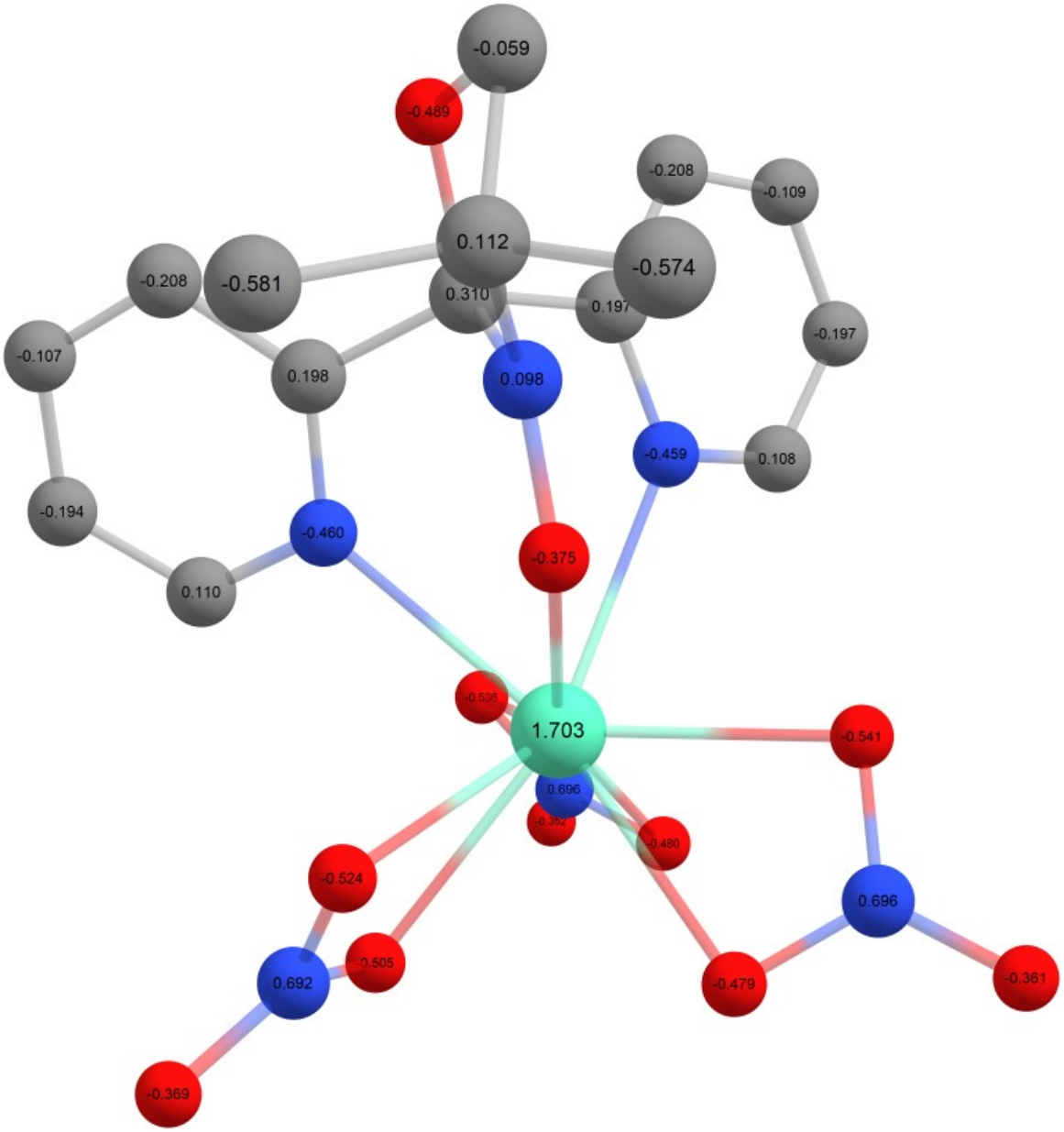

Figure S13. Natural charge distribution for [EuRad(NO_3)$_3$] calculated for he ground sextet at UB3LYP/def2-TZVP level with SARC2-DKH-QZVP basis set for Eu and relativistic DKH2 Hamiltonian.

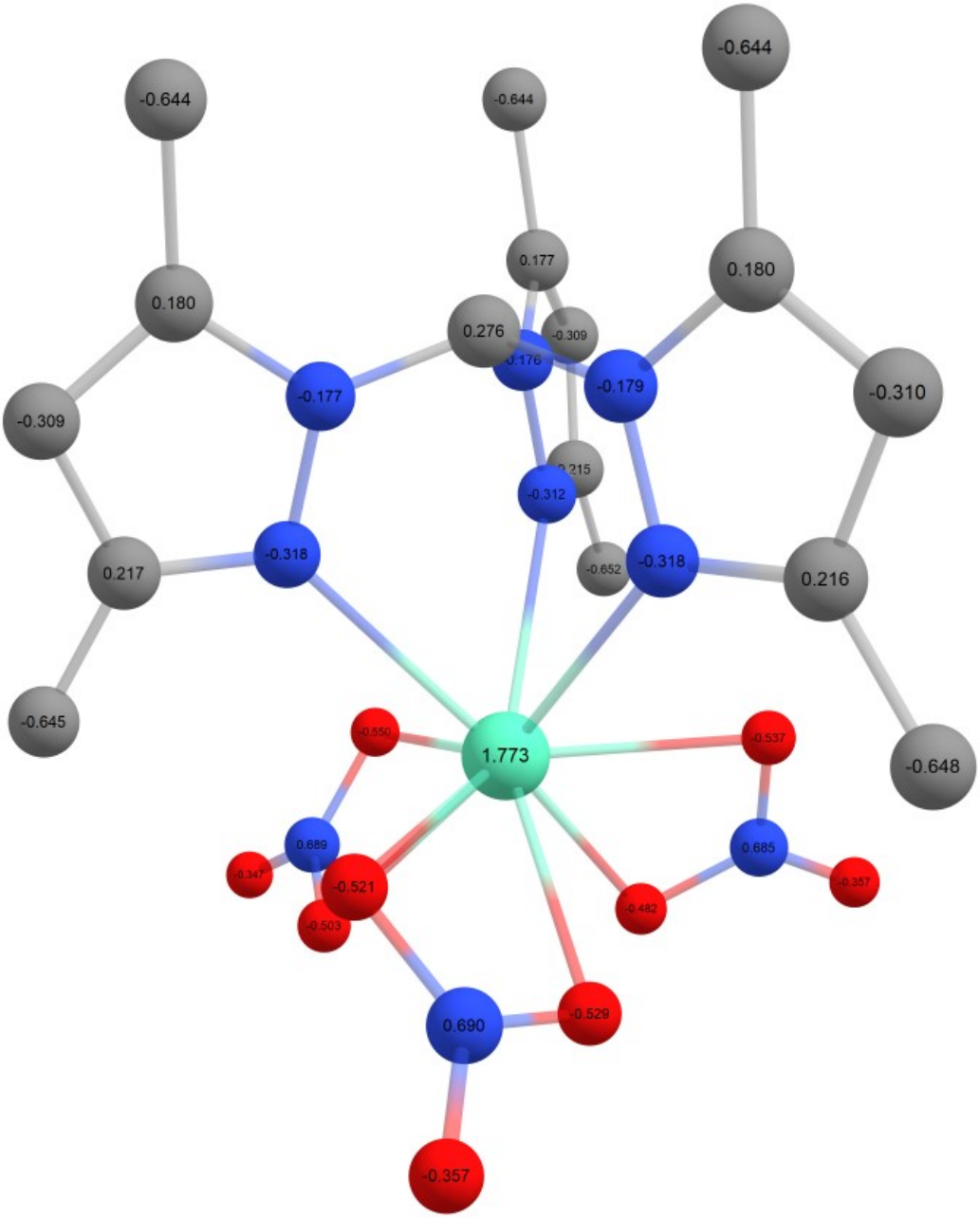

Figure S14. Natural charges distribution in [Eu(Tpm)(NO_3)$_3$] calculated in the ground septet at UB3LYP/def2-TZVP level with SARC2-DKH-QZVP basis set for Eu and relativistic DKH2 Hamiltonian.

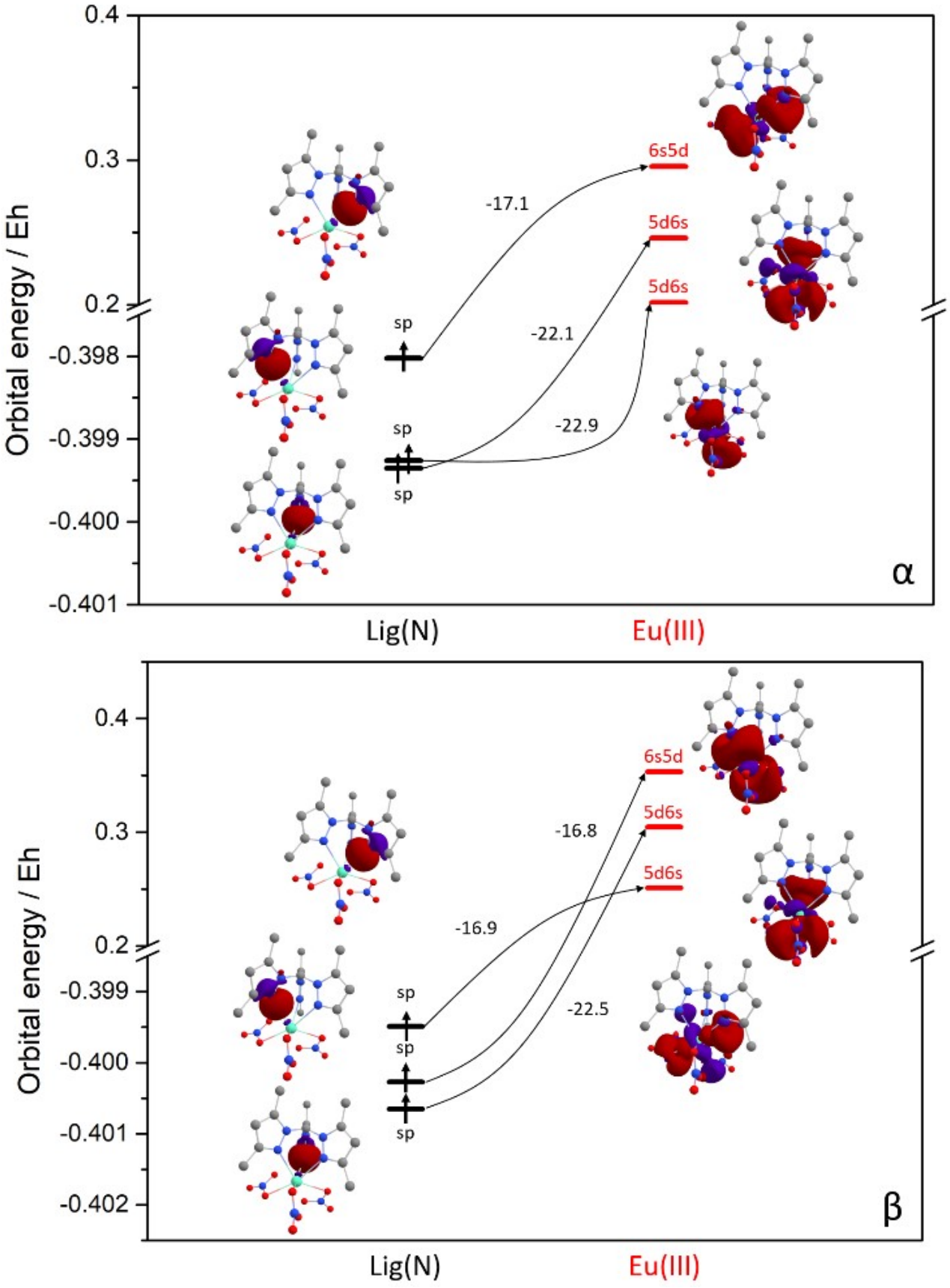

Figure S15. Orbital energy diagrams for the bond formation in the [Eu(Tpm)$(NO_3)_3$] complex between Eu^{3+} and L_{dia} ligand, the main electron donation paths are presented. The values of these individual components can be found in Table 2 (main text).

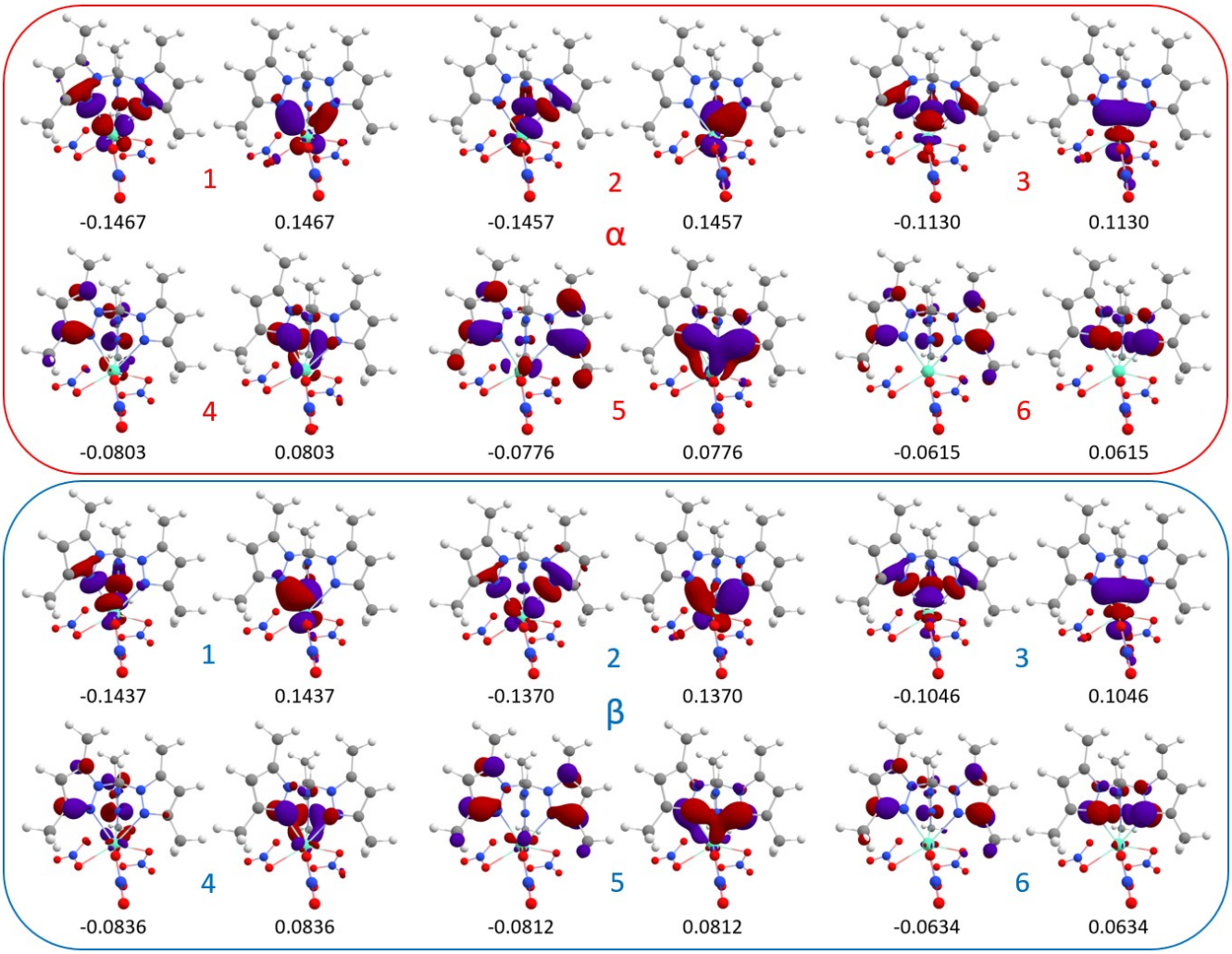

Figure S16. The most important pairs of α and β NOCVs responsible for σ (top row) and π (bottom row) type bonding in [Eu(Tpm)$(NO_3)_3$] complex with their eigenvalues. Each pair of NOCVs corresponds to two orbitals with positive and negative eigenvalues of the same magnitude.

Table S9. Contributions from the six most important NOCVs to ΔE_{orb} calculated for [EuRad$(NO_3)_3$] (**1**) and [Eu(Tpm)$(NO_3)_3$] (**2**) complexes in kJ mol^{-1}.

		1	**2**	**3**	**4**	**5**	**6**	ΔE_{orb} **(α or β)**
1	α	-33.5	-30	-18.1	-8.3	-5.2	-3.9	-132.5
	β	-33	-27.7	-16	-5.6	-6	-3.8	-123.1
2	α	-27.1	-26.7	-18.3	-5.2	-4.9	-3.3	-123.8
	β	-26.5	-24.8	-16.5	-5.6	-5.4	-3.5	-120.0

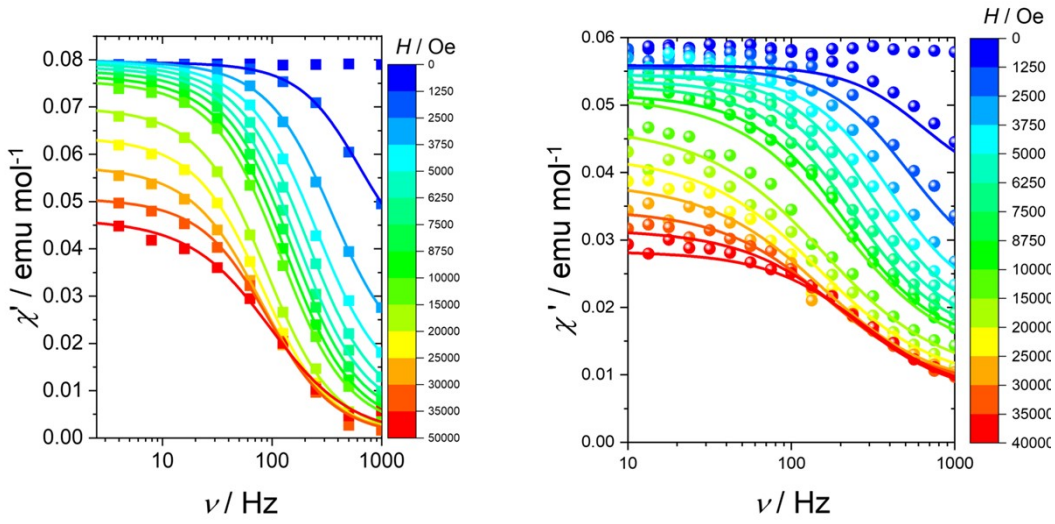

Figure S17. In-phase component of the ac magnetic susceptibility of Lu (left) and Eu (right). Field scan at T = 2 K.

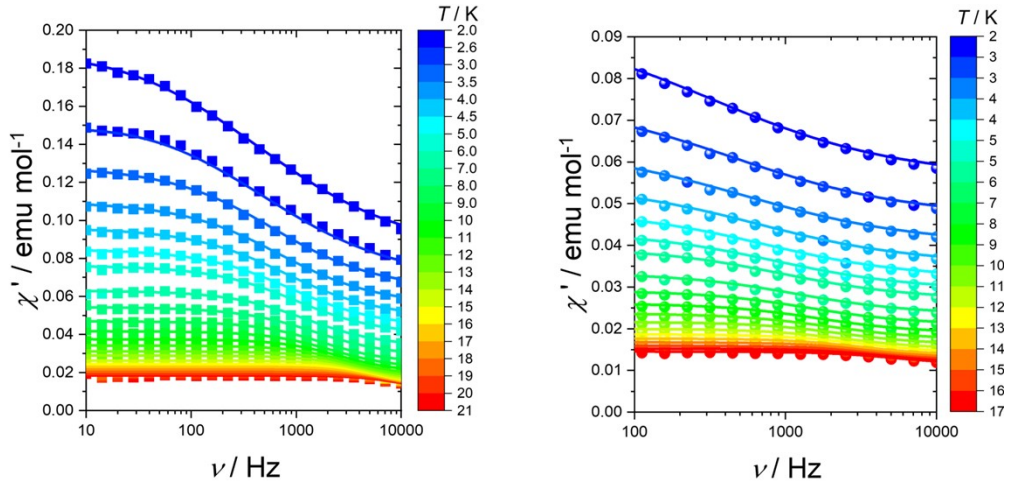

Figure S18. In-phase component of the ac magnetic susceptibility of Lu (left) and Eu (right). Temperature scan at H = 1000 Oe.

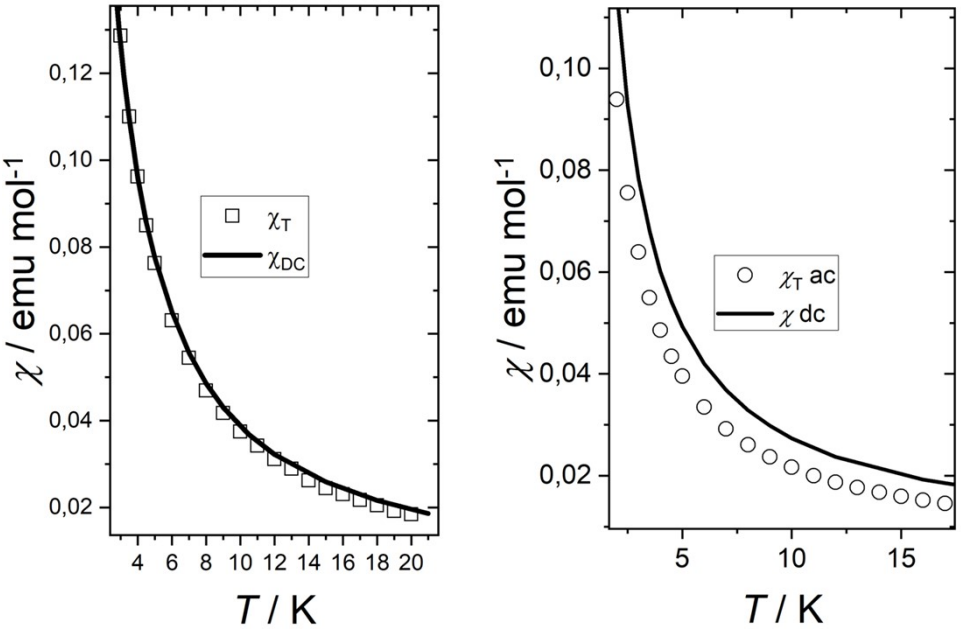

Figure S19. Comparison between the dc susceptibility and the isothermal value of the ac susceptibility obtained from the fit of the ac curves: **Lu** (left), **Eu** (right).